On the Magnification of Two-dimensional Contouring Errors by Using Contour-parallel Offsets

Soichi Ibaraki[1] * and Atsushi Matsubara[1]

[1] *Department of Micro Engineering, Kyoto University, Yoshida-honmachi, Sakyo-ku, Kyoto 606-8501, Japan*

Abstract

The cross grid encoder is a diffraction grating type encoder to measure two-dimensional position of a optical head by using a grid plate, and is widely used in the industry to evaluate the two-dimensional contouring performance of a machine tool. In the graphical display of measured contouring error profiles, the error is often magnified to some given scale with respect to the reference trajectory. The conventional algorithm to compute the magnified contouring error profile, adopted in a commercial software to analyze an error profile measured by the cross grid encoder, makes the magnified trajectory discontinuous when the given reference trajectory is unsmooth, which makes it difficult to understand the magnified trajectory especially at corners. This paper proposes a new algorithm to compute the magnified trajectory of two-dimensional contouring error profiles such that the magnified trajectory becomes continuous even when the reference trajectory is unsmooth. Application examples are presented with error profiles obtained by using a cross grid encoder applied to a commercial machining center.

Key words: Contouring Error, measurement, cross grid encoder, contour-parallel offset.

* Corresponding author. Phone/Fax: +81-75-753-5227
Email address: ibaraki@prec.kyoto-u.ac.jp (Soichi Ibaraki[1]).

1 Introduction

The international standards on the evaluation of static accuracies of machining centers, such as the ones described in ISO 230-1 and 10791-1∼4, basically define the machine's overall motion error as the accumulation of the motion error of each axis. The positioning error, straightness errors, or angular errors of each linear axis are independently measured, as well as the squareness error between two linear axes. On the other hand, accuracy calibration tests for a coordinate measuring machine (CMM), defined in ISO 10360 series, include error measurement with different concept. For a CMM, it is required to directly evaluate its three-dimensional positioning errors at given locations over the entire workspace by using, for example, the ball plate as an artefact. In recent years, the evaluation of volumetric accuracy has been considered more important even for machining centers, in order to ensure the motion accuracy over the entire three-dimensional workspace [1]. Currently, ASME B5 (TC52) and ISO 230 (TC39) are working on the standardization of the definition of volumetric accuracy [2].

The cross grid encoder is a diffraction grating type encoder to measure two-dimensional position of a optical head by using a grid plate where grids are aligned orthogonal to each other. The configuration of one of commercially available cross grid encoders, the KGM series by Dr. Johannes Heidenhain GmbH, is illustrated in Fig. 1 [3]. The cross grid encoder can measure the contouring error in the two-dimensional (2D) plane for an arbitrary reference trajectory. It is widely used in the accuracy calibration of robot manipulators [4] or machine tools [5]. Various types of other two-dimensional position encoders have been also proposed in the literature (e.g. [6]).

Since the 2D contouring error of a machine tool is generally much smaller in relative to the travelling distance, in its graphical display, the error is often magnified to some given scale with respect to the reference trajectory. Suppose that the given reference trajectory is represented by $\mathcal{R}$, and that the actual position of the target measured by using a cross grid encoder is given by $p(k) \in \mathbb{R}^2$ $(k = 1,\cdots,N)$. In commercial software to display 2D contouring errors, the magnification of contouring error is typically done by applying the

following simple algorithm (starting from $k = 1$):

(1) For the actual position $p(k)$, find the nearest point, $\tilde{r}(k)$, on the reference trajectory, $\mathcal{R}$.
(2) For the given magnification constant, $\eta \in \mathbb{R}$, plot the point at the location $\tilde{r}(k) + \eta \cdot (p(k) - \tilde{r}(k))$.
(3) $k \to k + 1$ and repeat from (1).

It is easy to see that this simple algorithm fails to make the magnified error trajectory continuous, when the reference trajectory is not smooth. As an illustrative example, consider the case where the reference trajectory is given as a square corner. The algorithm above is illustrated in Fig. 2. Since the point, $\tilde{r}(k)$, "jumps" at the point where $p(k)$ is in the same distance from both edges, it is clear that the magnified trajectory cannot be continuous at any unsmooth corners.

To further illustrate this issue, its application examples to experimental data are shown. When the reference trajectory is given as a square corner as shown in Fig. 3(a), the two-dimensional contouring error of a commercial vertical-type machining center is measured by using the cross grid encoder, KGM182 by Heidenhain. Figure 3(b) shows the measured trajectory of the spindle position within the small region shown in Fig. 3(a) (no magnification is made). It can be observed that there is a contouring error of about 60 μm at maximum at the corner, followed by a slight overshoot. Although it is easy on Fig. 3(b) to intuitively understand the measured error profile at this corner, this plot can only show a very small region. When it is needed to display the entire error trajectory, this plot is not suitable. The magnified plot, obtained by applying the conventional algorithm above, is shown in Fig. 3(c). It shows a "jump" due to the discontinuity of the magnified trajectory at the corner. As a result, it is very difficult to intuitively understand from this plot if there is an undershoot or an overshoot at the corner. ACCOM EN 2.8 [7], a commercial software by Dr. Johannes Heidenhain GmbH to be used with the KGM series for the data acquisition and the visual display of its measured profiles, gives the same plot.

Another example given in Fig. 4(a) shows an error profile measured experimentally by using the same cross grid encoder for the reference trajectory composed of segments and arcs [5] . Similarly, there are jumps due to the discontinuity of the magnified trajectory at all the corners. It is practically not possible to observe how the actual trajectory looks like at these corners.

Another potentially critical problem with the conventional magnification occurs when the reference trajectory is given as a series of small segments. When the reference trajectory contains a free-form curve, its NC program is typically given as a series of small straight segments. Figure 5(a) shows the magnified error profile measured experimentally by using the same cross grid encoder. The entire reference trajectory is given as a series of small straight segments of the length 0.1 mm. When the region indicated in Fig. 5(a) is zoomed in as shown in Fig. 5(b), it can be observed that the magnified profile has many "loops." Similarly as the jumps observed at corners, these loops indicate the discontinuity of the magnified profile.

To address these issues, this paper presents a new algorithm to compute the magnified trajectory of two-dimensional contouring error profiles.

2 Proposed algorithm to magnify contouring error profiles and its application examples

Suppose that the reference trajectory is represented by $\mathcal{R}$, and the measured position profile of the target is given by $p(k) \in \mathbb{R}^2$ $(k = 1,\cdots,N)$. The proposed algorithm to magnify the contouring error of the profile, $p(k)$, with respect to the reference trajectory, $\mathcal{R}$, is given as follows:

(1) Generate two contour-parallel trajectories by offsetting the reference trajectory, $\mathcal{R}$, to both sides of the trajectory by the given distance, $\delta \in \mathbb{R}$. This operation can be written by:

$$\begin{aligned} \mathcal{Q}_1 &= \text{offset}\,(\mathcal{R}, -\delta) \\ \mathcal{Q}_2 &= \text{offset}\,(\mathcal{R}, +\delta) \end{aligned} \tag{1}$$

where the function "offset$(\mathcal{R}, x)$" represents the computation of the trajectory that is generated by parallel offsetting the trajectory $\mathcal{R}$ by the

distance x.

(2) Starting from $k = 1$, find the point, $\tilde{q}(k)$, on either of the offset trajectories, $\mathcal{Q}_1$ and $\mathcal{Q}_2$, which is the closest to the point, $p(k)$.

(3) Compute the intersection point, $\tilde{r}(k)$, of the line connecting $p(k)$ and $\tilde{q}(k)$ and the reference trajectory $\mathcal{R}$.

(4) Plot the point at the location $\tilde{p}(k) := \tilde{r}(k) + \eta\,(p(k) - \tilde{r}(k))$, where $\eta \in \mathbb{R}$ is the given magnification constant. $k \to k + 1$ and repeat from (2).

For the computation of contour-parallel offsets, there have been numerous research efforts to build algorithms with higher robustness and smaller computational complexity [8]. In this paper, we adopt the algorithm developed by Held [9] to compute parallel offsets based on the Voronoi diagram.

As an illustrative example, Figure 6 shows the schematics of the proposed magnification applied to error trajectories at convex and concave corners. Unlike the conventional algorithm, in the square region of the size $\delta \times \delta$ at the corner, the error trajectory is magnified in a radial direction. As a result, the magnified trajectory becomes continuous even when the reference trajectory is unsmooth.

Note that the parameter, δ, must be set such that it is sufficiently larger than the maximum contouring error. Also note that as the parameter, δ, is larger, the region where the error profile is magnified to the radial direction becomes larger, as illustrated in Fig. 6.

The proposed algorithm is applied to three examples of the magnification of experimental error profiles presented in Section 1. Figure 3(d) shows the magnified error trajectory computed by applying the proposed algorithm to the same experimental profile shown in Fig. 3(c). Unlike Fig. 3(c), the magnified profile is continuous, and it can be observed that there is an undershoot of the magnitude about 60 μm at maximum at the corner, followed by an overshoot of the magnitude about 3 μm. Figure 4(b) shows the magnified error trajectory by applying the proposed algorithm to the same experimental profile shown in Fig. 4(a). Similarly, an overshoot at all the three corners can be more clearly observed. Figure 5(c) shows the case with the same experi-

mental profile shown in Fig. 5(a). As can be observed in the zoomed-in view in Fig. 5(d), there is no "loop" in the magnified error trajectory.

As illustrated in these examples, the proposed magnification exaggerates the error at a corner as a "spike," which may lead the misunderstanding of error geometry. It is to be noted that in the circular test, which is widely accepted in the industry for the calibration of machine tools, the "stick motion," or the quadrant glitch, one of the most common contouring errors observed in a circular test caused by the friction at quadrant changes [10], is observed as a spike in the magnified error plot. We expect that spikes observed in the proposed magnification can be similarly understood by an operator.

3 Conclusion

The proposed algorithm makes the magnified trajectory of two-dimensional contouring error profiles continuous, even when the reference trajectory is unsmooth. Especially at corners, and when the reference trajectory is given by a series of minute segments, the proposed algorithm can generate the magnified error trajectory that is much easier to intuitively understand than the one generated by the conventional algorithm. Application examples to error profiles experimentally obtained by using a cross grid encoder on a commercial machining center clearly indicate the effectiveness of the proposed algorithm.

References

[1] C. Wang, A Definition of Volumetric Error. *Manufacturing Engineering*, 134 (1), (2005).

[2] Svoboda, O., Bach P., Liotto, G., Wang, C. Definitions and correlations of 3D volumetric positioning errors of CNC machining centers. *The IMTS 2004 Manufacturing Conference*, (2004).

[3] S. Ibaraki, W. Goto, A. Matsubara, T. Ochi, M. Hamamura, Self-calibration of a cross grid encoder, *Journal of the Japan Society for Precision Engineering*, 72 (8), (2006), 1032–1037. (in Japanese)

[4] International Organization for Standardization (ISO), ISO/TR 13309:1995, Manipulating industrial robots – Informative guide on test equipment and metrology methods of operation for robot performance evaluation in accordance with ISO 9283, (1995).

[5] K. Lee, S. Ibaraki, A. Matsubara, Y. Kakino, Y. Suzuki, S. Arai, J. Braasch, A Servo Parameter Tuning Method for High-speed NC Machine Tools based on Contouring Error Measurement, *Laser Metrology and Machine Performance VI*, WIT Press, (2002).

[6] W. Gao, Precision nano-fabrication and evaluation of a large area sinusoidal grid surface for a surface encoder, *Precision Engineering*, 27, (2003), 289.

[7] ACCOM User's Manual (English) (2007/5), Dr. Johannes Heidenhain GmbH, (2007).

[8] D. Dragomatz, S. Mann, A Classified Bibliography of Literature on NC Milling Path Generation, *Computer Aided Design*, 29(3), (1997), 239–247.

[9] M. Held, VRONI: An Engineering Approach to the Reliable and Efficient Computation of Voronoi Diagrams of Points and Line Segments, *Computational Geometry: Theory and Application*, 18(2), (2001), 95–123.

[10] Kakino, Y., Ihara, Y., Shinohara, A., *Accuracy Inspection of NC Machine Tools by Double Ball Bar Method*, Hanser Publishers, 1993.

List of Tables

List of Figures

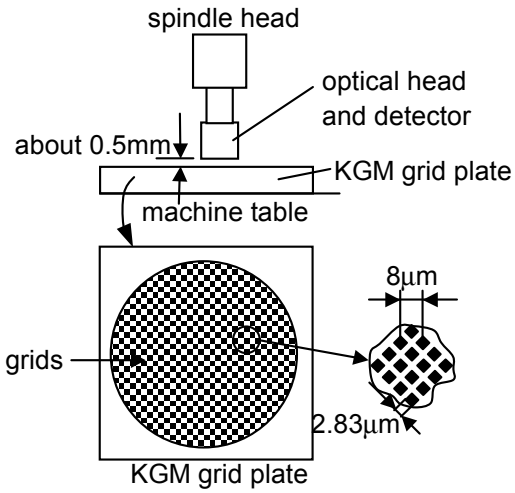

Fig. 1. A schematic view of a cross grid encoder [3].

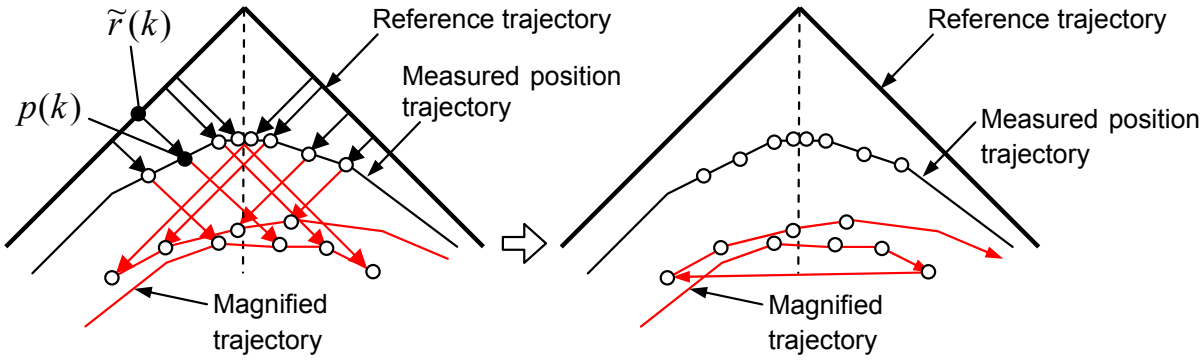

Fig. 2. Schematics of the conventional magnification of contouring error at a square corner.

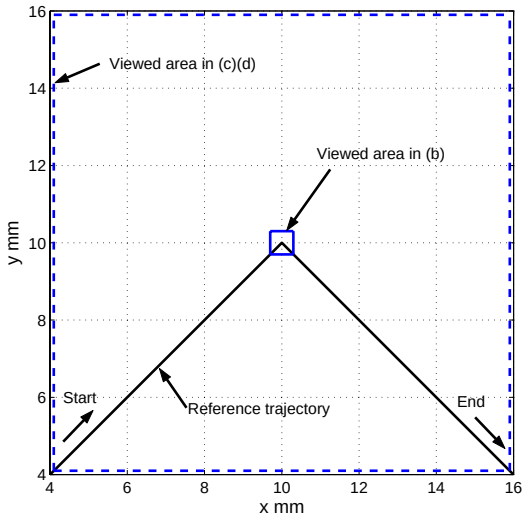

(a) Reference trajectory and areas viewed in (b) and (c)(d).

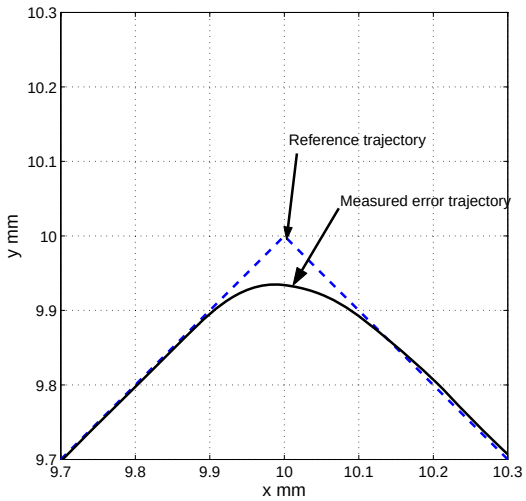

(b) Actual measured trajectory (the area indicated in (a) is zoomed).

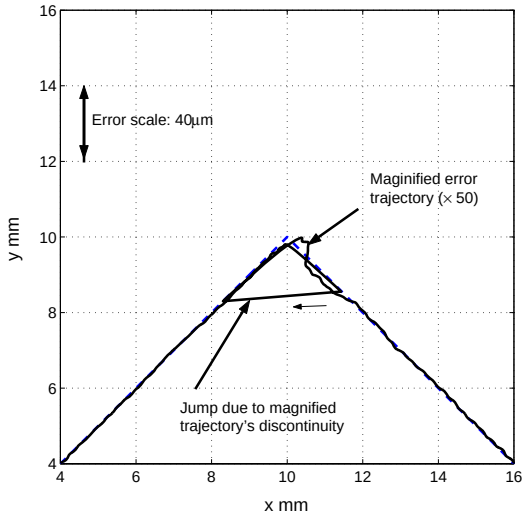

(c) Conventional magnification of error trajectory.

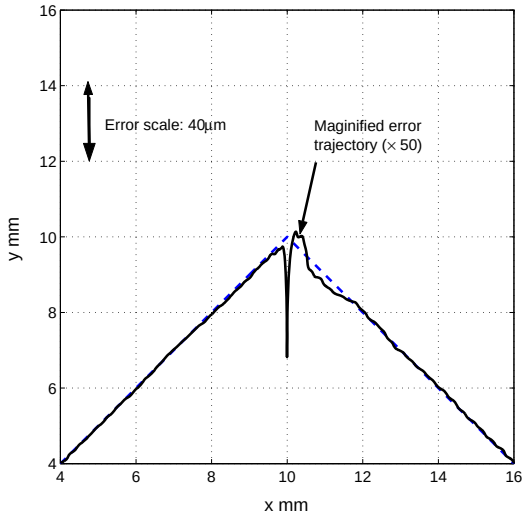

(d) Proposed magnification of error trajectory.

Fig. 3. An example of magnified error trajectories #1 (a square corner).

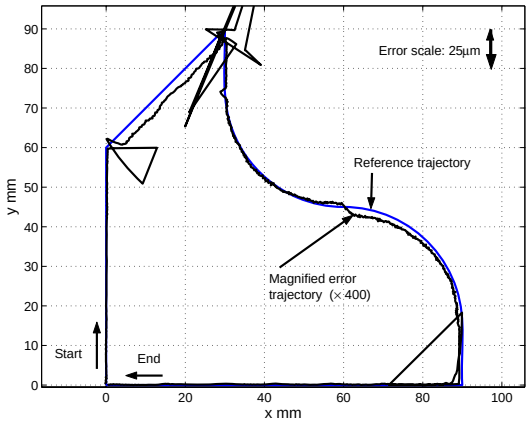

(a) Conventional magnification.

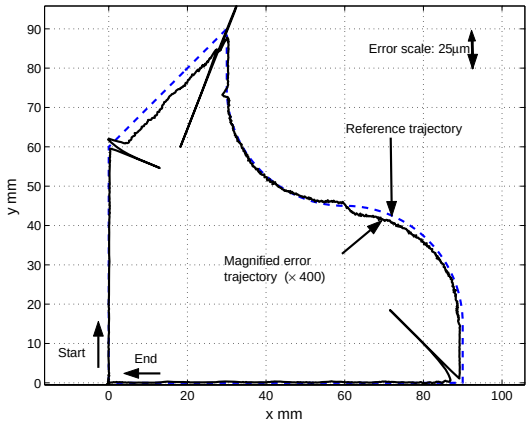

(b) Proposed magnification.

Fig. 4. An example of magnified error trajectories #2 (a reference trajectory consisting of segments and arcs).

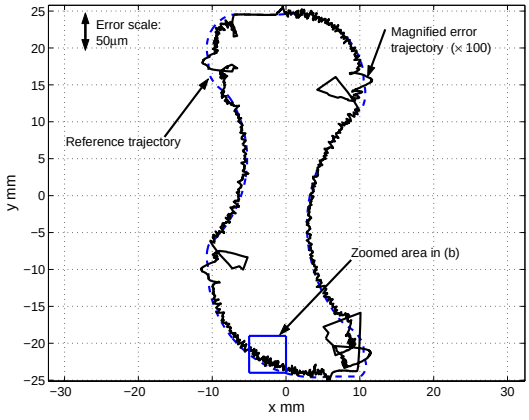

(a) Conventional magnification.

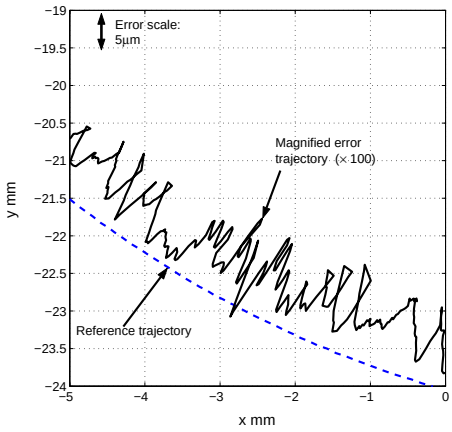

(b) Conventional magnification (the area indicated in (a) is zoomed in).

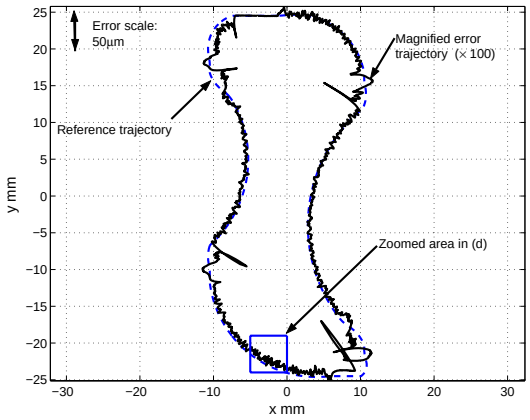

(c) Proposed magnification.

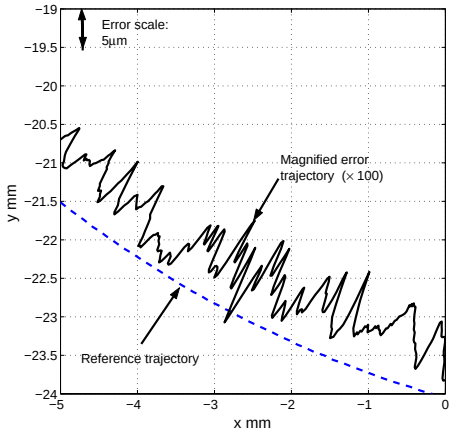

(d) Proposed magnification (the area indicated in (c) is zoomed in).

Fig. 5. An example of magnified error trajectories #3 (a reference trajectory given as a series of small segments).

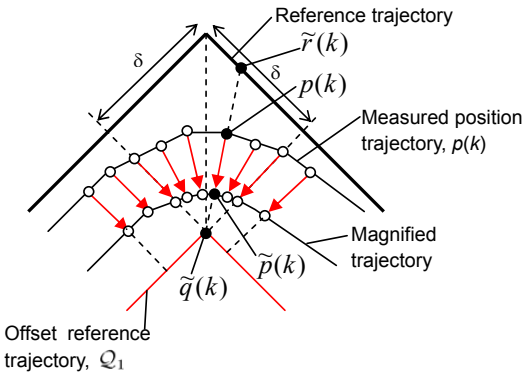

(a) For a convex reference trajectory.

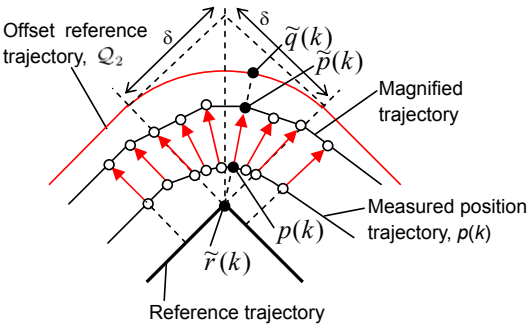

(b) For a concave reference trajectory.

Fig. 6. Schematics of the proposed magnification of contouring error at square corners.